CrossMark

Synthesis and biological studies of ^{99m}Tc(HYNIC–MFL)(tricine)(TPPTS) as a novel tumor imaging agent

J. Wang[1,2] · W. Yang[1,2] · J. Xue[1,2] · Y. Zhang[1,2] · W. Han[1,2] · Y. Liu[1,2]

Abstract This work reports the synthesis, radiolabeling and biological studies of ^{99m}Tc(HYNIC–MFL)(tricine) (TPPTS) in tumor-bearing mice. The novel melphalan derivative was successfully synthesized by conjugation of HYNIC to melphalan. The ligand could be labeled by ^{99m}Tc in high yield to get ^{99m}Tc(HYNIC–MFL)(tricine) (TPPTS), which was very hydrophilic and was stable at room temperature. Biodistribution studies in tumor-bearing mice showed that ^{99m}Tc(HYNIC–MFL)(tricine)(TPPTS) accumulated in the tumor with favorable uptake and retention. The good accumulation in tumor tissue, high tumor/ muscle ratios and satisfactory scintigraphic images highlight the potential of ^{99m}Tc(HYNIC–MFL)(tricine)(TPPTS) for tumor imaging.

Keywords ^{99m}Tc(HYNIC–MFL)(tricine)(TPPTS) · Melphalan · Label · Tumor imaging

The nitrogen mustards are an important class of DNA cross-linking agents, which are utilized in the treatment of many types of cancer [1]. The cytotoxicity of nitrogen mustards is due to their ability to alkylate DNA, RNA and proteins leading to the formation of DNA interstrand cross links [2, 3]. The prototype nitrogen mustard drug is mustine, which is no longer commonly in use. Other nitrogen mustards include cyclophosphamide, chlorambucil, uramustine, ifosfamide, melphalan and bendamustine.

Due to the tumor affinity of nitrogen mustards, they have been studied as potential tumor imaging agents after radionuclides labeling. D. Satpati et al. have reported a ^{99m}Tc(CO$_3$)-labeled chlorambucil analog which shows good tumor uptake of 3.2 ± 0.3 % ID/g at 3 h p.i. However, the complex is not stable in vivo [4]. Our previous studies have confirmed the ^{99m}Tc(CO)$_3$-labeled pegylated chlorambucil ([^{99m}Tc(CO)$_3$(IDA-PEG$_3$-CB)]$^-$, IDA = iminodiacetic acid) shows good accumulation in tumor tissue with high tumor/muscle ratios. Its major disadvantage lies in the slow clearance from normal organs [5]. Another ^{99m}Tc(CO)$_3$-labeled chlorambucil we have investigated is ^{99m}Tc(CO)$_3$(His-CB). It exhibits high initial tumor uptake with certain retention, fast clearance from background, good tumor/background ratios and satisfactory scintigraphic images, all of which highlight the potential of ^{99m}Tc(CO)$_3$(His-CB) as a tumor imaging agent [6]. Melphalan has been labeled with ^{125}I directly to get [^{125}I] Melphalan, which has a high affinity to be localized in the tumor site and meets most of the requirements necessary to be used as a successful diagnostic and therapeutic agent [7].

^{99m}Tc is the most widely used radionuclide for diagnostic imaging with SPECT because of its favorable physical properties ($t_{1/2}$ = 6 h, E_γ = 140 keV), low cost, and widespread availability [8]. In search for a more suitable ^{99m}Tc-labeled tumor imaging probe based on the biomolecule melphalan, 6-hydrazinonicotinyl (HYNIC) was chosen as the chelating agent because it has been widely used in ^{99m}Tc labeled proteins and peptides on the basis of different coligands [9–12]. The ^{99m}Tc-HYNIC labeling is very effective using very small amount of ligand

✉ J. Wang
wangjianjun@ihep.ac.cn

✉ Y. Liu
yuliu@ihep.ac.cn

1 Key Laboratory of Nuclear Radiation and Nuclear Energy Technology, Institute of High Energy Physics, Chinese Academy of Sciences, Beijing 100049, China

2 Beijing Engineering Research Center of Radiographic Techniques and Equipment, Beijing 100049, China

to form a stable result complex. For ^{99m}Tc-labeling, HYNIC was used as the bifunctional coupling agent whereas tricine and TPPTS (trisodium triphenylphosphine-3,3′,3″-trisulfonate) were used to stabilize the ^{99m}Tc-HYNIC core in ^{99m}Tc complex: ^{99m}Tc(HYNIC–MFL)(tricine)(TPPTS).

Experimental

Materials and methods

Melphalan was purchased from Sigma/Aldrich, China. Other reagents and solvents were from Beijing Chemical Reagents Company, China. All the chemicals were analytically pure and used without further purification. HYNIC–OSu (–OSu = –oxy succinimide) was synthesized according to the described method [13]. ^{1}H NMR spectra were recorded with a 500 MHz spectrometer by using TMS (tetramethylsilane) as the internal standard. Mass spectrometry was performed on a Bruker Daltonics esquire 6000 mass spectrometer with electrospray-ionisation prob. A ^{99}Mo/^{99m}Tc generator was obtained from the China Institute of Atomic Energy. Thin layer chromatography (TLC) was performed on a polyamide strip developed by dichloromethane/methanol = 1/1 (V/V). High performance liquid chromatography (HPLC) analysis was carried out by using a Hitachi LC2000 System with Bioscan FC3200 radio-detector. The column (Kromasil 100-5C18, 250 × 4.6 mm) was eluted at a flow rate of 1.0 mL/min. Water with 0.1 % trifluoroacetic acid (A) and methonal with 0.1 % trifluoroacetic acid (B) mixtures were used as the mobile phase and the following gradient elution technique was adopted for the preparation (0 min 10 % B, 15 min 40 % B, 20 min 90 % B, 25 min 10 % B). The imaging studies were performed with Eplus-166 small animal SPECT/CT system (Institute of High Energy Physics, Chinese Academy of Sciences).

Synthesis of the ligand (Fig. 1)

The HYNIC–melphalan conjugate (HYNIC–MFL) was synthesized by reacting HYNIC–OSu with an equivalent amount of melphalan. The reaction is schematically shown in Fig. 1. To 10 mL of N,N-dimethyl formamidine (DMF) were added HYNIC–OSu (192 mg, 0.5 mmol) and melphalan (163 mg, 0.5 mmol), followed by addition of 100 μL of triethylamine (Et$_3$N). The reaction mixture was stirred at room temperature over night. Then 10 mL of pure water was added. The precipitate was filtered, washed with DMF (0.1 mL) and ethanol (1 × 3 mL). The final product was collected and dried to give a yellow powder. The yield was 115 mg (40.2 %). ^{1}H NMR (500 MHz, DMSO): δ = 2.95 (s, 6 H), 3.02 (m, 2 H), 3.67 (m, 9 H), 4.45 (bs, 1 H), 5.59 (d, 1 H), 6.65 (d, 2 H), 6.74 (d, 2 H), 7.15 (m, 2 H), 7.51 (d, 2 H), 7.96 (m, 2 H), 8.40 (bs, 1 H), 8.56 (s, 1 H), 10.99 (s, 1 H), ppm. ESI-MS: 571.38 (MH$^+$), 593.71 (M + Na$^+$).

Radiosynthesis of ^{99m}Tc(HYNIC–MFL) (tricine)(TPPTS) (Fig. 2)

To a solution of 0.1 mL of DMSO and 0.5 mL of PBS (pH 6) were added 1 mg of HYNIC–MFL, 25 mg of tricine and 5 mg TPPTS (tris(3-sulfonatophenyl)phosphine, sodium salt). Stannous chloride (10 μL, 3 mg/mL, pH 1) was added followed by addition of freshly eluted ^{99m}Technetium pertechnetate (111 MBq; 100 μL). The reaction mixture was heated at 100 °C for 15 min. After cooling to room temperature, the radiochemical purity (RCP) of the complex was checked by TLC and HPLC.

Determination of the partition coefficient

The partition coefficient was determined by mixing the complex with an equal volume of 1-octanol and phosphate buffer (25 mM, pH 7.4) in a centrifuge tube. The mixture
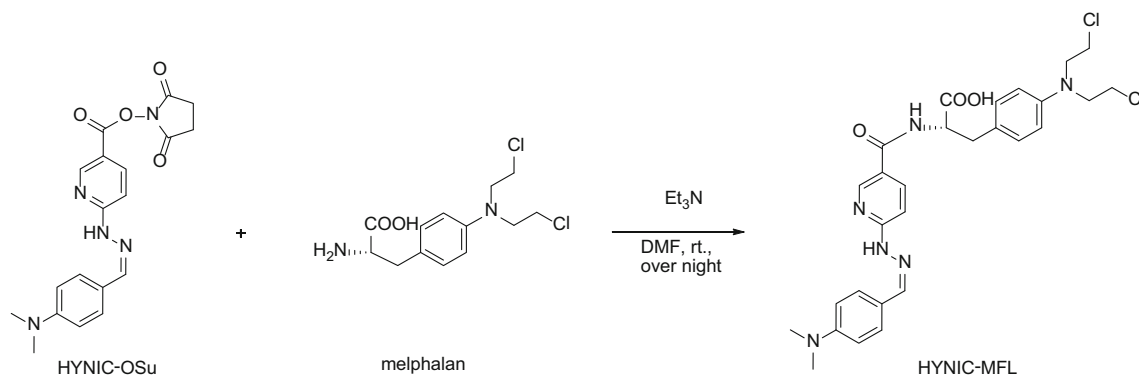

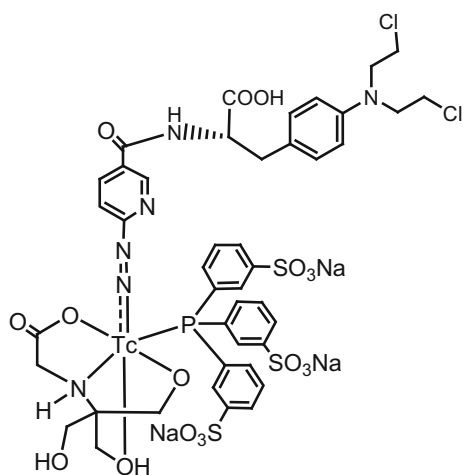**Fig. 1** Synthesis of the HYNIC–MFL

Fig. 2 The proposed structure of ^{99m}Tc(HYNIC–MFL)(tricine)-(TPPTS)

was vigorously stirred for 10 min at room temperature, and was then transferred to an Eppendorf microcentrifuge tube. The tube was centrifuged at 8000 rpm for 10 min. Samples in triplets from n-octanol and aqueous layer were obtained, and were counted in a well γ-counter. The partition coefficients were calculated using the following equation: $P =$ (activity in n-octanol)/(activity in aqueous layer). The final partition coefficient value was expressed as log P.

Stability studies

The room-temperature stability of the complex was determined by measuring the RCP at 25 °C at different time points (0, 1, 2, 4, 6 h) after preparation. Serum stability was determined by ^{99m}Tc(HYNIC–MFL)(tricine)(TPPTS) diluted 20-fold with freshly prepared murine serum, and the solutions were incubated at 37 °C for 6 h. At different time points (0, 1, 2, 4, 6 h), the serum was passed through a Sep-Pak C18 cartridge (waters), washed with 0.5 mL of water and eluted with 0.5 mL of acetonitrile containing 0.1 % trifluoroacetic acid. The combined aqueous and organic solutions were passed through a 0.22 μm Millipore filter and evaluated by radio-HPLC.

Biodistribution studies in tumor-bearing mice

Biodistribution characteristics of ^{99m}Tc(HYNIC–MFL)(tricine)(TPPTS) were evaluated using ICR mice bearing S180 cancer xenografts. In vivo growth was initiated by hypodermic injection of approximately 10^6 S180 cells into the left front leg of female ICR mice. Seven-eight days after inoculation, the tumor size was in the range of 0.5–0.8 g, and animals were used for biodistribution studies. A solution of the ^{99m}Tc(HYNIC–MFL)(tricine)(TPPTS) (100 μL, 185

KBq) was injected into the tumor-bearing mice ($n = 20$) via the tail vein. Five mice were sacrificed at 30, 60, 120 and 240 min post-injection (p.i.). The organs of interest and blood were collected, weighed and measured for radioactivity. The accumulated radioactivity in the tissue of organs was calculated in terms of percentage of injected dose per gram organ (%ID/g). The biodistribution data, tumor/muscle and tumor/blood ratios are reported as an average plus the standard variation. All biodistribution studies were carried out in compliance with the national laws related to the conduct of animal experimentation.

Imaging studies

The imaging studies of ^{99m}Tc(HYNIC–MFL)(tricine)(TPPTS) were performed using ICR mice bearing S180 cancer xenografts. A solution of the ^{99m}Tc(HYNIC–MFL)(tricine)(TPPTS) (100 μL, 14.8 MBq) was injected into the tumor-bearing mice via the tail vein. Multiple static scans were obtained at 30, 60, 120, 180, and 240 min p.i.

Results and discussion

Synthesis and radiosynthesis

Derivatization of melphalan to the suitable precursor was essential for subsequent ^{99m}Tc-labeling. ^{99m}Tc-HYNIC is a very attractive ^{99m}Tc-labeling core for its much high labeling efficiency and very stable result complex [9–12]. In order to get the HYNIC–melphalan ligand (HYNIC–MFL), HYNIC was activated by n-hydroxysuccinimide (HOSu) and then reacted with melphalan. HYNIC–MFL was precipitated and purified by solvents washing. The ^{99m}Tc-labeling of HYNIC–MFL was very effectively through a simple method. When TLC was performed, ^{99m}Tc(HYNIC–MFL)(tricine)(TPPTS) moved to the solvent front ($R_f = 0.8$–1.0), ^{99m}TcO$_2 \cdot n$H$_2$O remained at the origin ($R_f = 0$) and R_f value for ^{99m}TcO$_4^-$ was about 0.0–0.1. According to the TLC analysis, there was no observable ^{99m}TcO$_2 \cdot n$H$_2$O impurity in the radiolabeling results. The HPLC pattern of ^{99m}Tc(HYNIC–MFL)(tricine)(TPPTS) is shown in Fig. 3. It was observed that the retention time was found to be 7.64 min. The mean radiochemical purity (RCP) of the complex was over 95 % after the preparation.

Partition coefficient (log P)

The partition coefficient (log P) of ^{99m}Tc(HYNIC–MFL)(tricine)(TPPTS) was obtained to be -2.70 ± 0.03, suggesting that it had very good hydrophilicity.
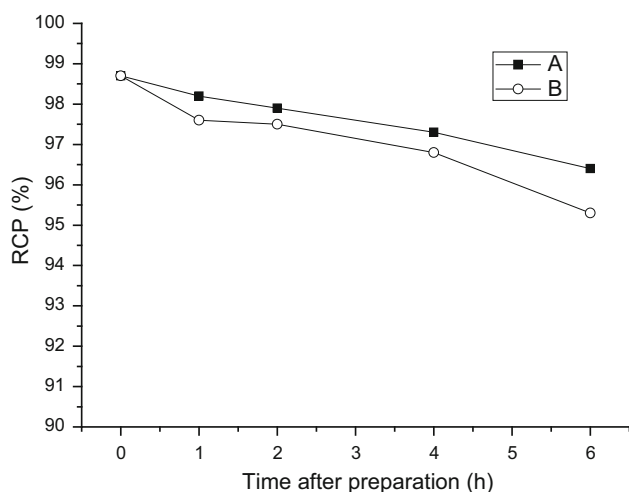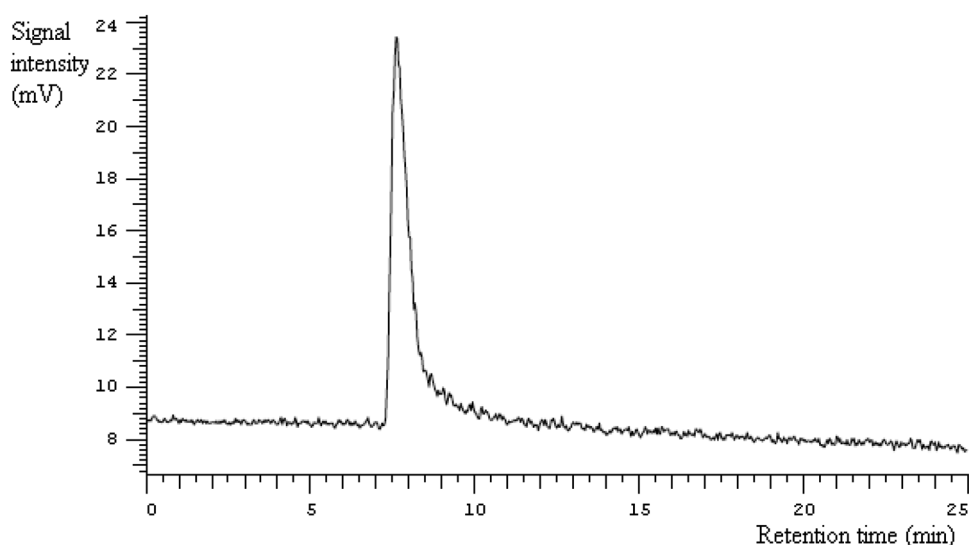
Fig. 3 HPLC pattern of ^{99m}Tc(HYNIC–MFL)(tricine)(TPPTS)

Fig. 4 The RCP curve of ^{99m}Tc-DTPA-CHC in the reaction mixture (A) or in serum (B) at different time points (0, 1, 2, 4, 6 h)

Table 1 Biodistribution study results of ^{99m}Tc(HYNIC–MFL)(tricine)(TPPTS) in tumor-bearing mice (ID %/g, $x \pm s$, $n = 5$)

Tissue	30 min	60 min	120 min	240 min
Tumor	1.83 ± 0.36	1.76 ± 0.55	1.12 ± 0.16	0.98 ± 0.37
Blood	3.12 ± 0.42	1.55 ± 0.14	0.80 ± 0.11	0.36 ± 0.05
Heart	0.99 ± 0.09	0.59 ± 0.08	0.41 ± 0.06	0.25 ± 0.01
Liver	2.63 ± 0.87	1.85 ± 0.15	1.68 ± 0.35	1.23 ± 0.27
Spleen	0.75 ± 0.03	0.50 ± 0.04	0.51 ± 0.11	0.38 ± 0.14
Lung	2.18 ± 0.17	1.42 ± 0.13	0.99 ± 0.14	0.62 ± 0.11
Kidneys	6.01 ± 0.73	5.41 ± 0.70	6.05 ± 1.20	5.07 ± 0.70
Brain	0.13 ± 0.05	0.10 ± 0.04	0.05 ± 0.01	0.03 ± 0.01
Muscle	0.68 ± 0.05	0.46 ± 0.07	0.25 ± 0.09	0.15 ± 0.02
Bone	0.98 ± 0.32	0.97 ± 0.37	1.27 ± 0.54	0.87 ± 0.25
T/M ratio	2.69 ± 0.30	3.80 ± 1.00	4.77 ± 1.33	6.63 ± 2.02
T/B ratio	0.59 ± 0.11	1.12 ± 0.28	1.42 ± 0.17	2.75 ± 1.08

Stability of the complex

The RCP of the product was nearly constant (>95 %) in the reaction mixture at room temperature or in serum at 37 °C over the observed period of 6 h (Fig. 4), suggesting that the complex possessed a great stability in vitro.

Biodistribution studies

The data of biodistribution are summarized in Table 1. ^{99m}Tc(HYNIC–MFL)(tricine)(TPPTS) did exhibit tumor affinity with good accumulation and retention (30 min: 1.83 ± 0.36, 60 min: 1.76 ± 0.55, 120 min: 1.12 ± 0.16, 240 min: 0.98 ± 0.37 ID %/g). The complex was mainly excreted via hepatobiliary and especially renal route. The clearance from normal organs (except of kidneys and liver) was very fast, leading to low background at 4 h p.i. (blood: 0.36 ± 0.05, heart: 0.25 ± 0.01, spleen: 0.38 ± 0.14, lung: 0.62 ± 0.11, muscle: 0.15 ± 0.02 ID %/g). It had favorite tumor/muscle (T/M) ratios that increased up to 4 h p.i. (30 min: 2.69 ± 0.30, 60 min: 3.80 ± 1.00, 120 min: 4.77 ± 1.33, 240 min: 6.63 ± 2.02). Due to the fast blood clearance, the tumor/blood (T/B) ratios were also improved during the observation period (30 min: 0.59 ± 0.11, 60 min: 1.12 ± 0.28, 120 min: 1.42 ± 0.17, 240 min: 2.75 ± 1.08).

Imaging studies

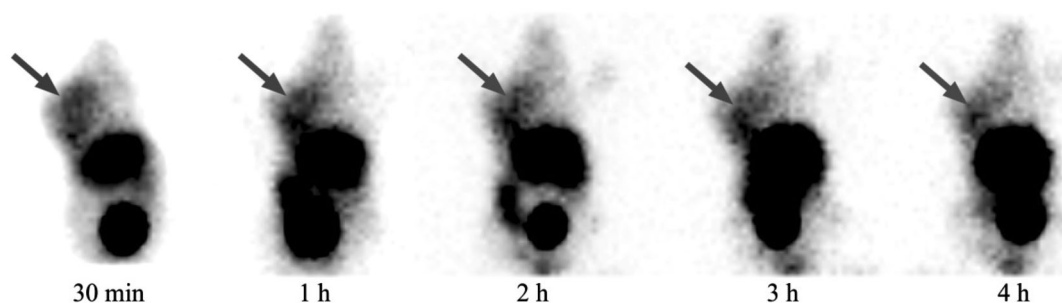In imaging studies, the tumor (indicated by arrows) was clearly visualized during the whole experiment with very

Fig. 5 Scintigraphic images with tumor-bearing mice after injection of ^{99m}Tc(HYNIC–MFL)(tricine)(TPPTS)

high tumor-to-muscle contrast (Fig. 5), which was consistent with the results from ex vivo biodistribution studies.

Conclusion

In this report, we have synthesized a new imaging agent ^{99m}Tc(HYNIC–MFL)(tricine)(TPPTS) showing substantial promise for tumor scintigraphy, as significant accumulation is observed in S180 tumor bearing mice. The RCP of the complex was over 95 %. It had good hydrophilicity and was stable at room temperature. ^{99m}Tc(HYNIC–MFL)(tricine)(TPPTS) showed obvious tumor uptake and retention, good tumor/muscle ratios and satisfactory scintigraphic images, suggesting it would be a promising candidate for tumor imaging.

References

1. Panasci L, Xu ZY, Bello V, Aloyz R (2002) Anticancer Drugs 13:211–220
2. Osborne MR, Wilman DEV, Lawley PD (1995) Chem Res Toxicol 2:316–320
3. Hurley LH (2002) Nat Rev Cancer 2:188–200
4. Satpati D, Korde A, Venkatesh M, Banerjee S (2009) Appl Radiat Isot 67(9):1644–1649
5. Wang J, Yang J, Yan Z, Duan X, Tan C, Shen Y, Wu W (2011) J Radioanal Nucl Chem 287:465–469
6. Wang J, Yang J, Duan X, Zhang Y, Yang W, Liu Y (2012) Bioorg Med Chem Lett 22:7406–7409
7. Amin AM, Soliman SE, El-Aziz HA (2010) J Label Compd Radiopharm 53:1–5
8. Jurisson SS, Lydon JD (1999) Chem Rev 99:2205–2218
9. Liu S, Edwards DS, Barrett JA (1997) Bioconjug Chem 8:621–636
10. Abrams MJ, Juweid M, TenKate CI, Schwartz DA, Hauser MM, Gaul FE, Fuccello AJ, Rubin RH, Strauss HW, Fischman AJ (1990) J Nucl Med 31:2022–2028
11. Masahiro O, Yasushi A, Takahiro M, Yasushi F, Kazuma O, Tomoya U, Tsuneo S, Junji K, Hideo S (2001) Nucl Med Biol 28(3):215–224
12. Steffens MG, Oosterwijk E, Kranenborg MHGC, Manders JMB, Debruyne FMJ, Corstens FHM, Boerman OC (1999) J Nucl Med 40:829–836
13. Harris TD, Sworin M, Williams N, Rajopadhye M, Damphousse PR, Glowacka D, Poirier MJ, Yu K (1999) Bioconjug Chem 10(5):808–814